High purity Ge-Sb-Se/S step index optical fibers

H. PARNELL,[1,2] D. FURNISS,[1] Z. TANG,[1] Y. FANG,[1] T. M. BENSON,[1] C. L. CANEDY,[3] C. S. KIM,[3] M. KIM,[4] C. D. MERRITT,[3] W. W. BEWLEY,[3] I. VURGAFTMAN,[3] J. R. MEYER,[3] AND A. B. SEDDON[1,*]

[1]*Mid-Infrared Photonics Group, George Green Institute for Electromagnetics Research, Faculty of Engineering, University of Nottingham, University Park, NG7 2RD, Nottingham, UK*
[2]*Currently at Granta Design, ANSYS, Cambridge, UK*
[3]*Code 5613, Naval Research Laboratory, Washington DC 20375, USA*
[4]*KeyW Corporation, Hanover MD 21076, USA*
[*]*angela.seddon@nottingham.ac.uk*

Abstract: Chalcogenide glasses are a promising group of materials for remote sensing applications. Two compositions from the Ge-Sb-Se/S system are investigated as core and cladding glasses in a step index fiber (SIF). Following thermomechanical and refractive index measurements, mid-infrared (MIR) light guiding is demonstrated through an 8 m length of SIF with a $Ge_{20}Sb_{10}Se_{70}$ at. % core and $Ge_{20}Sb_{10}Se_{67}S_3$ at. % cladding. Using a single distillation procedure, $Ge_{20}Sb_{10}Se_{70}$ at. % glass fibers are shown to have low optical loss across the 2 to 10 μm wavelength range with the lowest baseline loss shown as 0.44 dB/m at 6.4 μm.

1. Introduction

The mid-infrared (MIR) region of light, found between 3-25 μm wavelength [1], covers an important diagnostic tool known as the molecular fingerprint [2]. Due to the strong vibrational resonances of almost all organic species, MIR light offers a unique opportunity to study the key building blocks of biological tissues *via* a non-destructive spectroscopy technique [3]. This is particularly promising for several remote sensing applications, not least towards the *in-vivo* diagnosis of early-stage cancer. Since MIR absorption bands can be five orders of magnitude stronger than the overtones and combination vibrational absorption bands of the NIR region [4], it is easier to distinguish between the relevant and competing MIR features. Consequently, a raft of new MIR photonic components is now being developed, including passive optical fibers which will form the basis of an imaging probe.

As one of only a few materials transparent to MIR light, chalcogenide glasses have the additional benefit of being vitreous in nature *i.e.* making it possible for them to be fiber-drawn. Based on one or more of the chalcogen elements (S, Se or Te) [5], the ternary Ge-Sb-Se chalcogenide system is of particular interest for medical applications, as it is thought to be less toxic than its arsenic-containing counterpart [6]. Defined by 5-35 atomic % (at. %) Ge, 5-40 at. % Sb and the remainder Se [7], Ge-Sb-Se compositions exhibit robustness, relatively good thermal, mechanical and chemical properties and transparency across the 2-16 μm wavelength region [7–10]. It has already been shown that Ge-Sb-Se glasses, including those from the $Ge_xSb_{10}Se_{90-x}$ at. % system, are best described by their chemically ordered network model (CONM) [11], which often exhibits an extremum for a number of properties, such as glass transition temperature (T_g), density and refractive index (n) [6]. Due to this chemical threshold, it is often difficult to identify two compositions which have appropriate thermal and optical properties, particularly if a low numerical aperture (NA) is desired. Ou *et al.* [12] and Zhang *et al.* [13] recently

demonstrated successful coupling of Ge-Sb-Se/ Ge-Sb-Se and Ge-Sb-Se/Ge-Se (core/cladding) glasses, respectively, for supercontinuum generation. However, both SIFs had a high NA. For applications that require lower NA, Wang *et al*. [14] and Guery *et al*. [15] have shown that the substitution of Se for S, has little effect on the atomic glass structure and that any observed changes in physical properties are caused primarily by a difference in -S- and -Se- bond strengths. Consequently, with increasing S content in the Ge-Sb-Se/S glass system, both the linear and nonlinear refractive indices decrease, whilst the T_g and optical band gap increase [14].

For the chalcogenide optical fibers to perform at their optimum, they must be prepared with high purity. However, the MIR region of light also embraces a number of absorption bands relating to atmospheric impurities such as oxygen, hydrogen and carbon [16–18]. Therefore, to achieve low optical losses in Ge-Sb-Se/S SIFs, it is necessary to synthesize the glasses from high purity starting elements with subsequent distillation, all under high vacuum. In addition to the constituent elements, gettering chemicals such as Al and $TeCl_4$ are often introduced during the fabrication of high-purity chalcogenide glasses [19–21], so that [O] and [H] impurities are minimized, respectively.

This paper reports an initial investigation of two compositions from the $Ge_{20}Sb_{10}Se_{70-x}S_x$ at. % system and assesses their suitability to act as core and cladding glasses in a multimode, large core SIF. A distillation procedure was investigated, specifically for the core glass composition. In section 2 the experimental methods of glass melting and annealing are set out, as well as the distillation technique and methods of characterization of the glasses in terms of XRD (X-ray diffractometry), imaging and analytical SEM (scanning electron microscopy), and thermal analysis to measure: glass transition temperatures and the temperature coefficients of viscosity. The approach to measuring refractive index dispersion of the glasses is reported, together with the fiber drawing process and method of fiber loss characterization. In section 3 the results are discussed in terms of numerical aperture and zero dispersion wavelength of the SIF and the effect of glass distillation on fiber optical loss.

2. Experimental

2.1. Glass melting and annealing

All of the Ge-Sb-Se/S glasses investigated in this paper, were prepared *via* the traditional melt-quench technique [5]. Each chalcogenide glass was made within a vitreous silica ampoule (Multilab, UK), which was initially $HF_{aq.}$ (*aq.* is *aqueous*) etched and annealed to remove residual stress. Carbonaceous deposits and/or physi-sorbed or chemi-sorbed water on the silica ampoule's internal surface were also removed, by air and then vacuum baking at 10^{-5} Pa at 1000 °C for 6 hours each. Prior to batching, all Ge-Sb-Se/S glass melting was begun by purifying elemental Se (99.999%; Materion, ABSCO Materials), Sb (99.9999%, Cerac, ABSCO Materials) and S (99.999% Materion, ABSCO Materials) *via* a bake-out procedure to remove surface impurities. Although it may be possible to purify the surface of elemental Ge through techniques such as acid washing (although this may leave hydrogen impurities), it is technically difficult to purify Ge through the bake-out procedure since elemental Ge and Ge-oxides have low, and similar vapor pressures [22,23]. Therefore, as-bought Ge (99.999%, Materion, ABSCO Materials) was batched, with purified Se, Sb and S, straight into the prepared silica glass ampoule. All weighing and batching was carried out inside a dry nitrogen glovebox (MBraun 150B-G, ≤0.1 ppm O_2 and ≤0.1 ppm H_2O). For the Ge-Sb-Se glass used to investigate high-purity unstructured optical fibers, 1000 wt. ppm $TeCl_4$ (Alfa Aesar, UK) was also batched at this stage. Using an oxygen-propane (BOC gas) torch (Jencons' Junior Jet 7, UK), the silica glass ampoule and its contents were sealed under a vacuum of 10^{-3} Pa. Chalcogenide glass melting was carried out in a modified rocking furnace (Instron), during which the raw materials were slowly heated to 900 °C and homogenized for 24 hours. After cooling to 700 °C, the ampoule was removed from the furnace and the Ge-Sb-Se/S melt was quenched *in situ*, inside the ampoule, using an external nitrogen

(BOC) gas flow jetted at the exterior of the ampoule surface to cool its contents. Immediately after quenching, the ampoule, containing the Ge–Sb–Se/S product, was annealed at its onset-T_g from differential scanning calorimetry (DSC) [24] for 0.5 hours and then allowed to cool to room temperature.

2.2. Ge-Sb-Se distillation

Following the initial melting and annealing of homogenized Ge-Sb-Se + 1000 wt. ppm $TeCl_4$, this chalcogenide glass boule was broken into approximately 2-5 mm diameter pieces and batched into the charged end of a silica glass distillation rig (Multilab, UK), which had been prepared *via* the same procedure outlined in section 2.1. Once again, batching was carried out within the dry nitrogen glovebox. At the same time, 700 wt. ppm Al (Alfa Aesar, UK) was also batched with the Ge-Sb-Se + 1000 wt. ppm $TeCl_4$ pieces so to act as a [O] getter during subsequent heating. Through careful temperature control, the charged end of the silica glass distillation rig was heated to approximately 700 °C. Ge-Sb-Se glass distillation occurred in an open system, under a drawing vacuum.

2.3. Glass characterization

X-ray diffractometry (XRD) was used to analyze the amorphous nature of the chalcogenide glasses using a Siemens D500 diffractometer, with CuKα radiation in the 2θ range 10°- 70°, and with a step size of 0.05°; 40 seconds was spent at each step, resulting in a run time of 13.2 hours. The onset-T_g was measured using differential scanning calorimetry (DSC) on 20 mg of as-annealed Ge-Sb-Se/S chunks, with dimensions ≤2 mm, in sealed aluminum pans. Each DSC sample was run 3 times in a Perkin Elmer Pyris 1 DSC analyzer, under flowing Ar gas and with a heating and cooling rate of 10 °C/min. The mean onset-T_g value (to ± 2 °C) was calculated from both the second and third runs. Viscosity-temperature measurements were carried out using a modified parallel plate technique, in a Perkin Elmer TMA7 thermomechanical equipment with flowing He (BOC) at 20 ml/min. A constant load of 50 mN was applied to samples with dimensions of 1.6 mm height and 4.7 mm diameter, whilst 400 mN was applied to samples with dimensions of 4.1 mm height and 4.7 mm diameter. Scanning electron microscopy (SEM), conducted on a FEI Philips XL30 SEM, was used to image Ge-Sb-Se/S samples under the backscattered electron (BSE) mode. When combined with energy dispersive X-ray spectroscopy (EDX), using Oxford Instruments INCA Energy software, the compositions of carbon-coated Ge-Sb-Se/S samples were measured with an accuracy of approx. ±0.5 at. % for elements heavier than oxygen.

2.4. Fiber-drawing and characterization of Ge-Sb-Se/S glass fibers

All of the Ge-Sb-Se/S optical fibers presented in this paper, were drawn from bulk glass preforms, which had been prepared *via* various techniques. Unstructured Ge-Sb-Se fibers were directly drawn from as-annealed glass rods (~70 mm long and 10 mm diameter). Unstructured Ge-Sb-Se-S fiber was drawn from a 4.7 mm diameter, ~90 mm long glass rod which had been extruded from an as-annealed 15 mm diameter boule [25]. Ge-Sb-Se/S SIF was drawn from a co-extruded 10 mm diameter preform [25] comprising a Ge-Sb-Se core and Ge-Sb-Se-S cladding. Both the Ge-Sb-Se core and Ge-Sb-Se-S cladding glasses used for this co-extrusion, were as-annealed 29 mm diameter glass boules which had been polished to a 1 μm finish on the mating surfaces. Extrusions were carried out using an in-house built, vertical extruder, under flowing N gas. Fiber-drawing took place on a customized Heathway draw-tower (housed in a class 10,000 cleanroom), during which the draw-zone was purged using nitrogen gas (BOC) which had been freeze-dried as it traveled through a copper-coil immersed in liquid nitrogen at 77 K. The chalcogenide preforms were softened and drawn to fiber using a short graphite ring-receptor, which was heated by radio frequency from a copper coil.

Optical fiber loss measurements were conducted on fiber samples ~7-18 m in length and $200 \pm 10\,\mu m$ diameter, *via* the cut-back method [26]. Using two set-ups, the optical fiber attenuation was first measured using an InSb cooled detector (JUDSON, UK) in the 2-5.5 µm wavelength range and then an MCT (HgCdTe) cooled detector (Kolmar Technologies, UK) in the 5-10 µm wavelength range. Both measurements were made with a Globar source and a KBr beam splitter. So that the peaks of impurity bands could be estimated, optical fiber loss measurements were also conducted on a shorter length (approx. 0.5 m) of the same fiber under investigation.

Thin film refractive index samples were prepared from 20 mm lengths of $200 \pm 10\,\mu m$ diameter unstructured $Ge_{20}Sb_{10}Se_{70}$ at. % and $Ge_{20}Sb_{10}Se_{67}S_3$ at. % optical fibers, which had been hot-pressed between two tungsten carbide plates, under vacuum (10^{-4} Pa) at T_g +40 °C (viscosity 10^8 Pa.s) with a maximum pressure of 700 N. Thin films were annealed at the onset-T_g and allowed to cool *in-situ*. Using an improved Swanepoel method, with a two-term Sellmeier model, refractive index measurements were found across the 2-25 µm MIR region and had an accuracy of <0.4% and standard deviation of precision < ±0.002. This accuracy was determined using a 3.1 µm interband cascade laser (ICL) [27,28] fabricated at NRL (which emitted >200 mW cw at 25 °C) by comparison with a benchmark refractive index value obtained from prism measurements on $Ge_{20}Sb_{10}Se_{70}$ at. % core and $Ge_{20}Sb_{10}Se_{67}S_3$ at. % cladding glasses. Both the thin film and prism refractive index samples were taken from the same batch. A full description of the improved Swanepoel method can be found elsewhere [29].

3. Results and discussion

3.1. Ge-Sb-Se/S step-index fibers

Following the work by Parnell *et al.* [11], prospective core and cladding compositions were chosen from the $Ge_{20}Sb_{10}Se_{70-x}S_x$ atomic % (at. %) chalcogenide glass system. With an overall aim of producing low NA SIFs, for greater selectivity in a future MIR imaging probe application, $Ge_{20}Sb_{10}Se_{70}$ at. % was selected as the core glass and $Ge_{20}Sb_{10}Se_{67}S_3$ at. % as the cladding. For the $Ge_{20}Sb_{10}Se_{70-x}S_x$ at. % glasses specifically relevant to this work, it was predicted that a 3 at. % substitution of Se for S would result in a 3 ± 1 °C increase in T_g and a 0.02 ± 0.01 decrease in refractive index [14]. Well matched T_gs are required for the co-processing of core and cladding glasses to fabricate the SIF. Using DSC analysis, the onset-T_g of each composition was measured and is presented in Table 1. From this Table, the $Ge_{20}Sb_{10}Se_{70}$ at. % core glass exhibits an onset-T_g of 214 °C, while the $Ge_{20}Sb_{10}Se_{67}S_3$ at. % cladding glass has an onset-T_g of 224 °C. This ΔT of 10 °C was larger than the predicted 3 °C, yet is particularly promising when considering the very large change in onset-T_g values when 5 at. % Se is substituted for Ge in the Ge-Sb-Se ternary glasses, *viz.*: $Ge_{15}Sb_{10}Se_{75}$ at. % (160.1 °C), $Ge_{20}Sb_{10}Se_{70}$ at. % (214 °C) and $Ge_{25}Sb_{10}Se_{65}$ at. % (316 °C) [30].

Table 1. Thermal properties of prospective $Ge_{20}Sb_{10}Se_{70}$ at. % core and $Ge_{20}Sb_{10}Se_{67}S_3$ at. % cladding glasses[a].

Composition / at. %	Glass transition temperature (T_g) /°C	Extrusion temperature (at $10^{7.5}$ Pa.s) /°C	Fiber-drawing temperature (at $10^{4.5}$ Pa.s) /°C
$Ge_{20}Sb_{10}Se_{70}$	214	274.7 ± 0.4	357.8 ± 0.7
$Ge_{20}Sb_{10}Se_{67}S_3$	224	277.7 ± 0.4	361.9 ± 0.3

[a] Note that T_g values were determined by means of DSC, whilst the extrusion and fiber-drawing processing temperatures were determined via viscometry using a TMA (see Fig. 1).

As well as studying the T_g of the core and cladding glasses, thermomechanical analysis was conducted to investigate the viscoelastic behavior associated with the extrusion and fiber-drawing process. Figures 1(a) and (b) present the full viscosity-temperature curves for the

$Ge_{20}Sb_{10}Se_{70}$ at. % core and $Ge_{20}Sb_{10}Se_{67}S_3$ at. % cladding glasses, respectively; the average viscosity-temperature results for the extrusion and fiber-drawing processes are presented in Table 1.
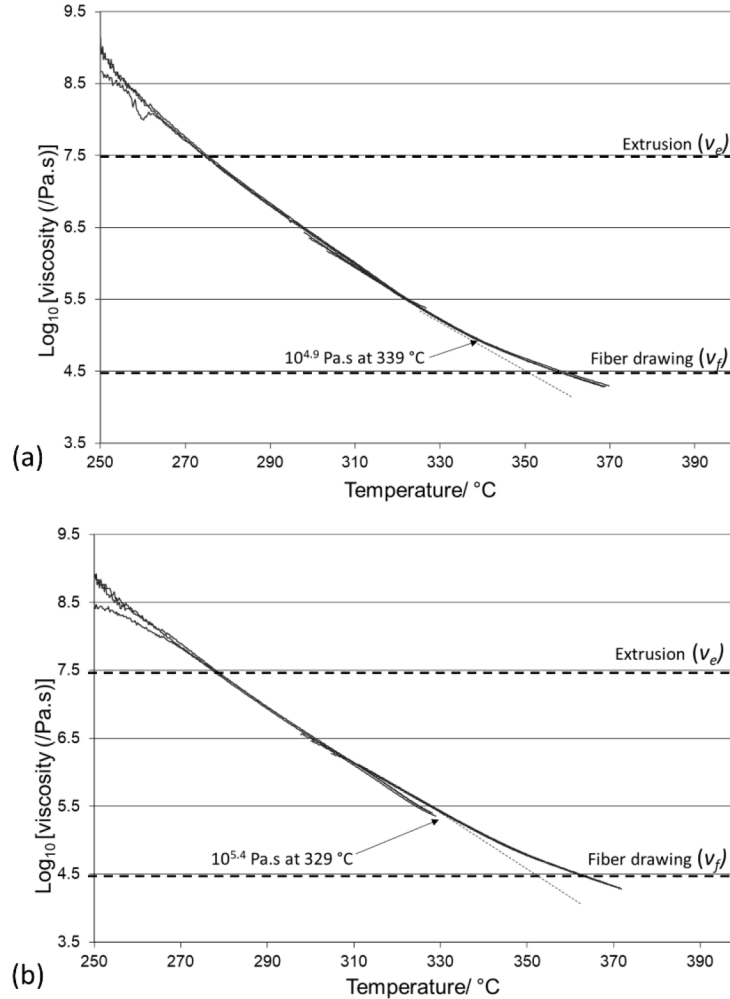
Fig. 1. Viscosity-temperature curves of the: a) $Ge_{20}Sb_{10}Se_{70}$ at. % core and b) $Ge_{20}Sb_{10}Se_{67}S_3$ at. % cladding glasses. Horizontal dashed lines indicate the approximate extrusion ($10^{7.5}$ Pa.s) and fiber-drawing ($10^{4.5}$ Pa.s) viscosities, denoted by v_e and v_f respectively. The dashed tangent lines indicate the onset of deviation from the linear fall of the viscosity-temperature curves.

Since the quality of the test piece can significantly impact the accuracy of the TMA viscometry results, the Ge-Sb-Se/S samples were carefully prepared from a 4.7 mm diameter, extruded rod, along which several cuts were made perpendicular to the rod axis. For both compositions, three cylindrical samples were cut with heights of 1.6 mm and another three with heights of 4.1 mm. The two sample geometries allowed the full range of the viscosity-temperature curves to be measured, considering sample spreading. Figure 1, presents the viscosity-temperature curves for all six samples. At relevant extrusion ($10^{7.5}$ Pa.s) and fiber-drawing ($10^{4.5}$ Pa.s) viscosities, the temperature was recorded for each sample curve. Therefore, the values presented in Table 1 are an average result calculated from three samples. Corresponding errors indicate the associated

standard deviation. Since the errors were found to be small, they are presented only in Table 1 and not in Fig. 1.

Results showed that the temperature required to reach the estimated extrusion viscosity of $10^{7.5}$ Pa.s was similar for both the $Ge_{20}Sb_{10}Se_{70}$ at. % core (274.7 ± 0.4 °C) and the $Ge_{20}Sb_{10}Se_{67}S_3$ at. % cladding (277.7 ± 0.4 °C) glasses. Likewise, the temperature required to achieve a fiber-drawing viscosity of approx. $10^{4.5}$ Pa.s was also close, with a ΔT of 4 °C between $Ge_{20}Sb_{10}Se_{70}$ at. % core (357.8 ± 0.7 °C) and the $Ge_{20}Sb_{10}Se_{67}S_3$ at. % cladding (361.9 ± 0.3 °C). These results suggest that the two prospective compositions have similar thermal coefficients of viscosity above T_g and should, therefore, successfully co-extrude.

A final observation is that both viscosity-temperature curves show a slight deviation from linearity, at 339 °C for the $Ge_{20}Sb_{10}Se_{70}$ at. % core and at 329 °C for the $Ge_{20}Sb_{10}Se_{67}S_3$ at. % cladding. This change in slope indicates a deviation from Arrhenian behavior, and possibly the breaking of different bonds on the atomic level.

In Fig. 2, the refractive index measurements of the $Ge_{20}Sb_{10}Se_{70}$ at. % core and $Ge_{20}Sb_{10}Se_{67}S_3$ at. % cladding glasses are shown from 2 to 25 µm wavelength. Overall, the dispersion curves presented in Fig. 2 show that the substitution of 3 at. % Se for S in the $Ge_{20}Sb_{10}Se_{70-x}S_x$ at. % system reduces the refractive index of the glass. At 3.1 µm wavelength, the $Ge_{20}Sb_{10}Se_{70}$ at. % core thin film had a refractive index of 2.553 whilst the cladding $Ge_{20}Sb_{10}Se_{67}S_3$ at. % thin film had a refractive index of 2.540. With a refractive index difference of approx. 0.01, also observed by Wang *et al.* [14], a SIF composed of a $Ge_{20}Sb_{10}Se_{70}$ at. % core and $Ge_{20}Sb_{10}Se_{67}S_3$ at. % cladding would give an NA of 0.25 at 3.1 µm wavelength. Ideally, SIFs in a hyperspectral imaging probe might have a slightly higher NA for superior light gathering. However, tailoring the Ge-Sb-Se/S compositions for higher NA, would in turn tend to increase detrimentally the difference in thermal properties.
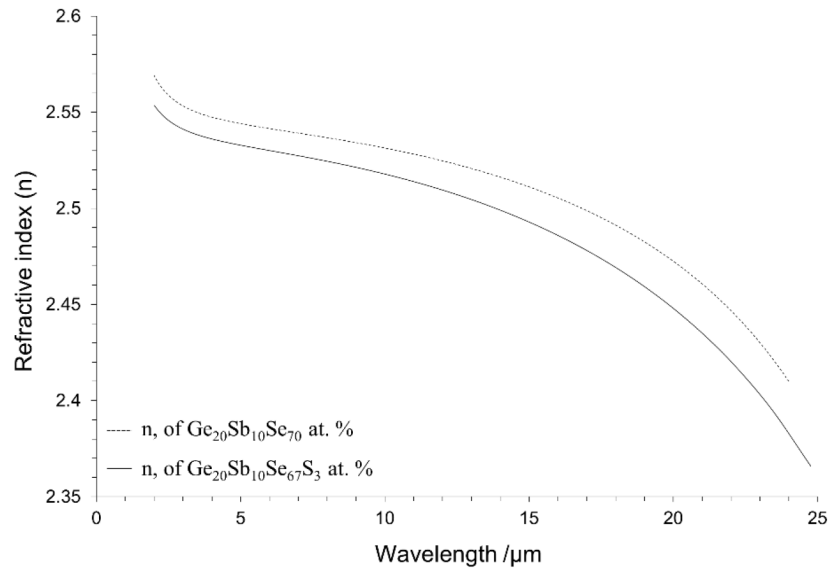
Fig. 2. Refractive index (n) measurements of $Ge_{20}Sb_{10}Se_{70}$ at. % core glass (dashed line) and $Ge_{20}Sb_{10}Se_{67}S_3$ at. % cladding glass (solid line).

Based on the refractive index measurements presented in Fig. 2, the calculated NA for the $Ge_{20}Sb_{10}Se_{70}$ at. % core and $Ge_{20}Sb_{10}Se_{67}S_3$ at. % cladding glasses is presented as a function of wavelength in Fig. 3 (a), along with the material dispersion in Fig. 3(b). Since the MIR long-wavelength fundamental vibrational absorption bands of the $Ge_{20}Sb_{10}Se_{67}S_3$ at. % cladding

is at a shorter wavelength than that of the $Ge_{20}Sb_{10}Se_{70}$ at. % core, the refractive index dispersion of $Ge_{20}Sb_{10}Se_{67}S_3$ at. % decreases faster than the $Ge_{20}Sb_{10}Se_{70}$ at. %. For this reason, the predicted NA increases with wavelength and from Fig. 3 (a), the lowest calculated NA (0.24) is at 4.7 µm whilst the highest (0.36) is at 23 µm wavelength. From Fig. 3 (b), the $Ge_{20}Sb_{10}Se_{70}$ at. % core and $Ge_{20}Sb_{10}Se_{67}S_3$ at. % cladding thin films have zero dispersion at 6.7 µm and 6.1 µm wavelengths, respectively.
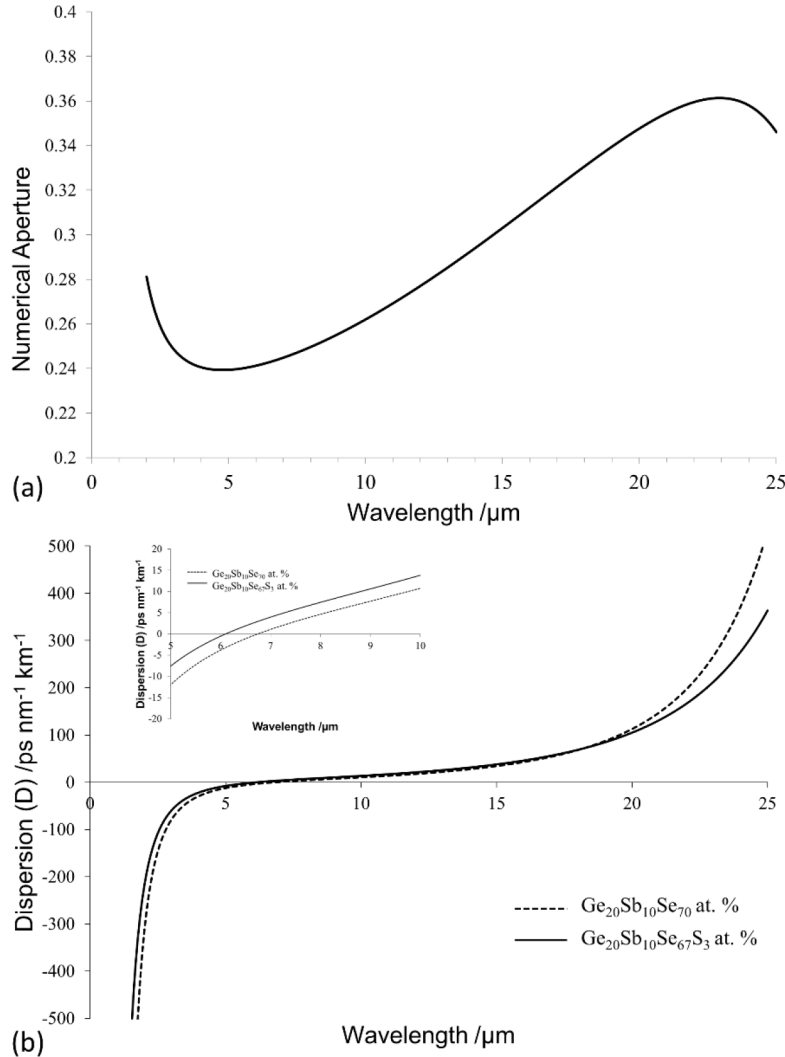
Fig. 3. (a) Calculated numerical aperture (NA) values for a step-index fiber (SIF) with $Ge_{20}Sb_{10}Se_{70}$ at. % core glass and $Ge_{20}Sb_{10}Se_{67}S_3$ at. % cladding glass. (b) Material dispersion (D) for a SIF with $Ge_{20}Sb_{10}Se_{70}$ at. % core and $Ge_{20}Sb_{10}Se_{67}S_3$ at. % cladding glasses. Inset shows an enlarged region between 5 to 10 µm.

Following these individual investigations of the $Ge_{20}Sb_{10}Se_{70}$ at. % core and $Ge_{20}Sb_{10}Se_{67}S_3$ at. % cladding glasses, both glass melts were combined for co-processing, firstly *via* a co-extrusion and then fiber-drawing to a 200 ± 5 µm diameter SIF. The optical fiber-loss was measured in an ~8 m length of this SIF (see Fig. 4), along with the individual fiber-losses of unclad $Ge_{20}Sb_{10}Se_{70}$ at. % core and $Ge_{20}Sb_{10}Se_{67}S_3$ at. % cladding glasses for comparison. Since none of the

chalcogenide glasses had been purified beyond an initial bake-out procedure, relatively large impurity bands were expected and found *e.g.*, the Se-H feature at 4.5 µm (10.51 dB/m) and Ge-O at 7.9 µm (19.05 dB/m). However, the absorption bands proved effective in demonstrating successful waveguiding in the SIF, as follows.
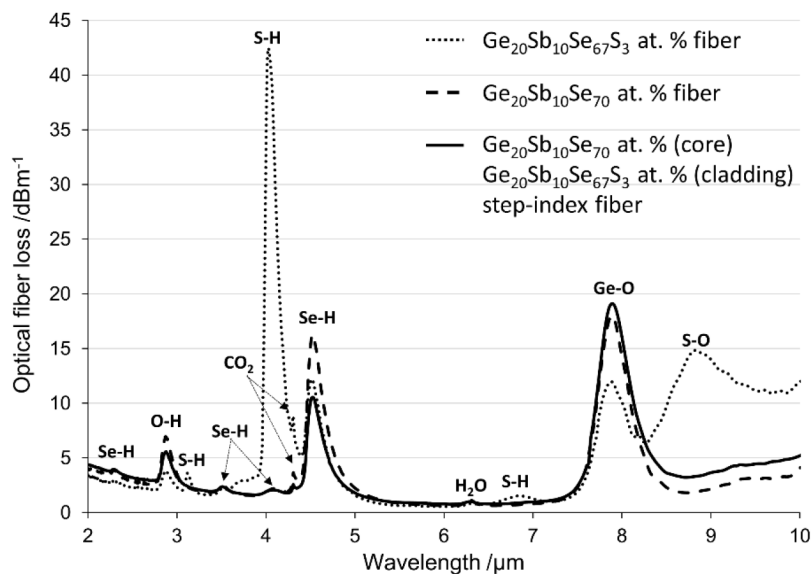
Fig. 4. Combined optical fiber loss measurements for unstructured $Ge_{20}Sb_{10}Se_{70}$ at. % core, unstructured $Ge_{20}Sb_{10}Se_{67}S_3$ at. % cladding and a $Ge_{20}Sb_{10}Se_{70}$ at. % (core) $Ge_{20}Sb_{10}Se_{67}S_3$ at. % (cladding) step-index fiber (SIF).

When light travels in a SIF, some portion of the optical mode inevitably occupies the cladding due to the evanescent wave phenomenon. Therefore, it was anticipated that traces of the $Ge_{20}Sb_{10}Se_{67}S_3$ at. % cladding impurity bands *e.g.* S-H at 4.04 µm (42.0 dB/m) and S-O at approx. 8.85 µm (14.8 dB/m), would show in the SIF fiber-loss results. However, as demonstrated in Fig. 4, there is very little difference between the SIF fiber-loss and that of the unstructured $Ge_{20}Sb_{10}Se_{70}$ at. % fiber. The absence of impurity vibrational absorptions associated with the $Ge_{20}Sb_{10}Se_{67}S_3$ at. % glass suggests that there was a successful mismatch between the refractive indices of the $Ge_{20}Sb_{10}Se_{70}$ at. % core and $Ge_{20}Sb_{10}Se_{67}S_3$ at. % cladding glasses, which promoted efficient propagation through the SIF core, accompanied by relatively weak evanescent field penetration into the cladding glass. The lowest loss for the $Ge_{20}Sb_{10}Se_{70}$ at. % core and $Ge_{20}Sb_{10}Se_{67}S_3$ at. % cladding SIF was measured as 0.72 dB/m at 6.06 µm wavelength.

To confirm the presence of a core-cladding structure, SEM-EDX analysis was conducted on SIF cleaves used for the fiber-loss measurements in Fig. 4. From a backscattered electron SEM image, presented in Fig. 5 (a), two distinct regions can be identified, compromising a large circular core and a 10 µm thick cladding. With an overall SIF diameter of 200 µm, the core to cladding ratio was found to be 95%. Using SEM-EDX, each region was confirmed as a $Ge_{20.4}Sb_{10}Se_{69.6}$ ±0.5 at. % core and a $Ge_{20.4}Sb_{9.9}Se_{66.5}S_{3.2}$ ±0.5 at. % cladding *i.e.* close to that nominally batched. Furthermore, the elemental mapping of S, as presented in Fig. 5 (b), shows a homogenous cladding in the SIF.

3.2. Low optical loss Ge-Sb-Se fibers

To minimize the optical absorption bands associated with oxygen, hydrogen and/or carbon, a distillation procedure was developed. Focusing on the $Ge_{20}Sb_{10}Se_{70}$ at. % core glass, 1000 ppm
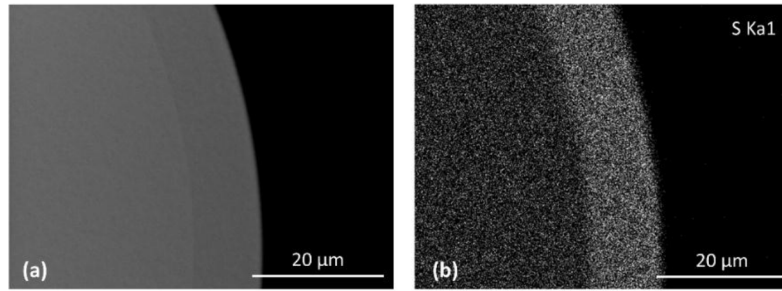
Fig. 5. a) Scanning electron microscopy (SEM) image of a cleaved optical fiber taken from the $Ge_{20}Sb_{10}Se_{70}$ at. % (core) $Ge_{20}Sb_{10}Se_{67}S_3$ at. % (cladding) step-index fiber and b) energy dispersive X-ray spectroscopy (EDX) map for elemental S (K lines used).

wt. $TeCl_4$ and 700 ppm wt. Al were added, to act as [H] and [O] getters, respectively. With adequate temperature control, the $Ge_{20}Sb_{10}Se_{70}$ at. % glass was shown to distil successfully at temperatures close to 693 °C in an open system, under a drawing vacuum. Following a re-melt at 900 °C for 10 hours the, nominally batched, distilled $Ge_{20}Sb_{10}Se_{70}$ at. % glass was quenched and annealed, before being drawn into 200 ± 10 µm diameter, uncladded fiber.

The optical fiber loss measurement presented in Fig. 6, for an 18 m section of the distilled $Ge_{20}Sb_{10}Se_{70}$ at. % glass (solid line), shows remarkably low loss across the 3-8 µm region: 0.62 ± 0.19 dB/m. The lowest baseline loss was measured as 0.44 dB/m at 6.42 µm wavelength. Although a small Se-H absorption can be seen at 4.6 µm, it is considered extremely difficult to remove all hydrogen impurities [31] and even the purest reported chalcogenide glasses exhibit a small [H] spectral absorption band centered at 4.6 µm [26,32,33]. To the best of the Authors' knowledge, this result is currently the lowest loss reported to date for Ge-Sb-Se optical fibers. To highlight the improved MIR transparency, the optical loss spectrum for the undistilled
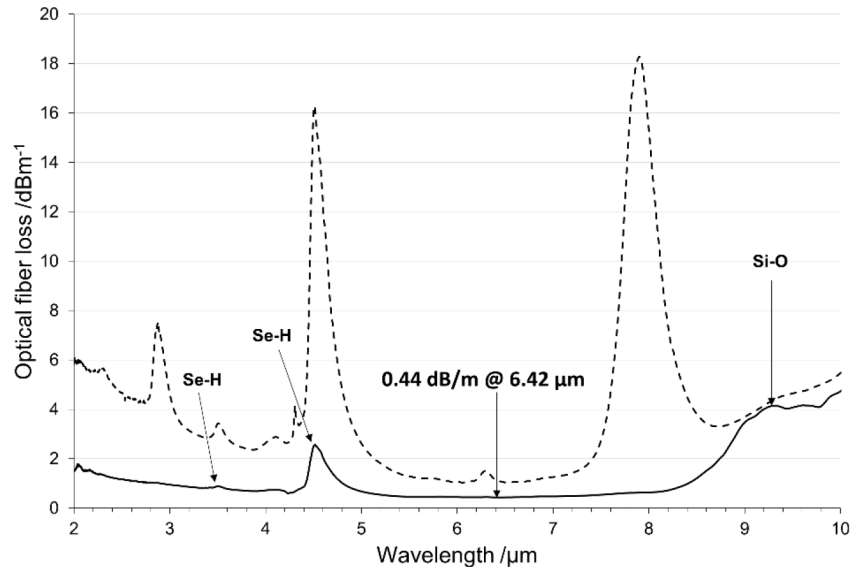
Fig. 6. Optical fiber loss spectra for the unstructured, distilled $Ge_{20}Sb_{10}Se_{70}$ at. % glass measured over an 18 m length of 200 µm diameter fiber (solid line). The optical loss in the undistilled $Ge_{20}Sb_{10}Se_{70}$ at. % optical fiber is included for comparison (dashed line).

$Ge_{20}Sb_{10}Se_{70}$ at. % optical fiber (presented in Fig. 4), is shown for comparison as the dashed line in Fig. 6. These results show that distilling the $Ge_{20}Sb_{10}Se_{70}$ at. % glass with [O] and [H] getters significantly reduces the Se-H and Ge-O absorption bands.

Using SEM-EDX, the chemical composition of the distilled $Ge_{20}Sb_{10}Se_{70}$ at. % glass was confirmed as $Ge_{21.1}Sb_{10.6}Se_{68.3}$ ±0.5 at. % (*cf.* as batched: $Ge_{20}Sb_{10}Se_{70}$). This measurement and standard deviation were based on several EDX points taken at regular intervals along the full 18 m length of the optical fiber. Although the final distilled glass composition did not exactly match that of the nominally-batched $Ge_{20}Sb_{10}Se_{70}$ at. % glass, the standard deviation of the EDX measurements indicate good homogeneity of the glass.

4.   Conclusions

Two compositions from the $Ge_{20}Sb_{10}Se_{70-x}S_x$ at. % glass system have been combined successfully to produce SIFs with low NA. Using DSC and TMA, it was found that the prospective $Ge_{20}Sb_{10}Se_{70}$ at. % core glass and the $Ge_{20}Sb_{10}Se_{67}S_3$ at. % cladding glass, had similar thermal properties. To achieve an extrusion viscosity of $10^{7.5}$ Pa.s there was a 3 °C temperature difference between the $Ge_{20}Sb_{10}Se_{70}$ at. % core glass (274.7 ± 0.4 °C) and the $Ge_{20}Sb_{10}Se_{67}S_3$ at. % cladding glass (277.7 ± 0.4 °C). Likewise, to achieve a fiber-drawing viscosity of $10^{4.5}$ Pa.s there was a 4 °C temperature difference between the $Ge_{20}Sb_{10}Se_{70}$ at. % core glass (357.8 ± 0.7 °C) and the $Ge_{20}Sb_{10}Se_{67}S_3$ at. % cladding glass (361.9 ± 0.3 °C). Furthermore, the measured refractive indices of 2.553 ($Ge_{20}Sb_{10}Se_{70}$ at. %) and 2.540 ($Ge_{20}Sb_{10}Se_{67}S_3$ at. %) at 3.1 μm wavelength gave a predicted SIF NA of 0.25. The zero dispersion wavelengths were also calculated to be 6.7 μm and 6.1 μm for the $Ge_{20}Sb_{10}Se_{70}$ at. % core and $Ge_{20}Sb_{10}Se_{67}S_3$ at. % cladding glasses, respectively. The two compositions were successfully drawn into a large core SIF, with the lowest optical baseline loss measured as 0.72 dB/m at 6.06 μm wavelength. To improve further the optical loss, a distillation procedure was developed specifically for high-purity $Ge_{20}Sb_{10}Se_{70}$ at. % optical fibers. Using Al as an [O] getter and $TeCl_4$ as a [H] getter, pre-homogenized $Ge_{20}Sb_{10}Se_{70}$ at. % glass was successfully distilled at temperatures close to 693 °C. Optical loss measurements made on an 18 m length of unstructured, nominally-batched $Ge_{20}Sb_{10}Se_{70}$ at. % fiber, drawn from the remelted distillate, revealed a remarkably low loss of 0.62 ± 0.19 dB/m across the 3-8 μm region. The lowest baseline loss of 0.44 dB/m, at 6.42 μm wavelength, appears to indicate that the Ge-Sb-Se fiber has the highest purity reported to date.

Funding

Acknowledgments

References

1. A. B. Seddon, "A Prospective for New Mid-Infrared Medical Endoscopy Using Chalcogenide Glasses," Int. J. Appl. Glass Sci. **2**(3), 177–191 (2011).
2. M. J. Baker, E. Gazi, M. D. Brown, J. H. Shanks, P. Gardner, and N. W. Clarke, "FTIR-based spectroscopic analysis in the identification of clinically aggressive prostate cancer," Br. J. Cancer **99**(11), 1859–1866 (2008).
3. A.B. Seddon, "Mid-infrared photonics for early cancer diagnosis," in *16th International Conference on Transparent Optical Networks (ICTON)*, Graz, 2014, pp.1–4.
4. P. W. France, M. G. Drexhage, J. M. Parker, M. W. Moore, S. F. Carter, and J. V. Wright, *Fluoride Glass Optical Fibres* (CRC Press, Inc, 1990).

5. A. B. Seddon, "Chalcogenide glasses: A review of their preparation, properties and applications," J. Non-Cryst. Solids **184**, 44–50 (1995).

6. W. H. Wei, L. Fang, X. Shen, and R. P. Wang, "Transition threshold in $Ge_xSb_{10}Se_{90-x}$ glasses," J. Appl. Phys. **115**(11), 113510 (2014).

7. J. A. Savage, P. J. Webber, and A. M. Pitt, "An assessment of Ge-Sb-Se glasses as 8 to 12μm infra-red optical materials," J. Mater. Sci. **13**(4), 859–864 (1978).

8. A. R. Hilton and D. J. Hayes, "The interdependence of physical parameters for infrared transmitting glasses," J. Non-Cryst. Solids **17**(3), 339–348 (1975).

9. M. Frumar, H. Tichá, J. Klikorka, and P. Tomíška, "Optical absorption in vitreous $GeSb_2Se_4$," J. Non-Cryst. Solids **13**(1), 173–178 (1973).

10. M. D. Rechtin, A. R. Hilton, and D. J. Hayes, "Infrared transmission in Ge-Sb-Se glasses," J. Electron. Mater. **4**(2), 347–362 (1975).

11. H. Parnell, D. Furniss, Z. Tang, N. C. Neate, T. M. Benson, and A. B. Seddon, "Compositional dependence of crystallization in Ge–Sb–Se glasses relevant to optical fiber making," J. Am. Ceram. Soc. **101**(1), 208–219 (2018).

12. H. Ou, S. Dai, P. Zhang, Z. Liu, X. Wang, F. Chen, H. Xu, B. Luo, Y. Huang, and R. Wang, "Ultrabroad supercontinuum generated from a highly nonlinear Ge-Sb-Se fiber," Opt. Lett. **41**(14), 3201–3204 (2016).

13. B. Zhang, Y. Yu, C. Zhai, S. Qi, Y. Wang, A. Yang, X. Gai, R. Wang, Z. Yang, and B. Luther-Davies, "High Brightness 2.2-12 μm Mid-Infrared Supercontinuum Generation in a Nontoxic Chalcogenide Step-Index Fiber," J. Am. Ceram. Soc. **99**(8), 2565–2568 (2016).

14. R. Wang, Q. Xu, H. Liu, Y. Sheng, and X. Yang, "Structure and physical properties of $Ge_{15}Sb_{20}Se_{65-x}S_x$ glasses," J. Am. Ceram. Soc. **101**(1), 201–207 (2018).

15. G. Guery, J. D. Musgraves, C. Labrugere, E. Fargin, T. Cardinal, and K. Richardson, "Evolution of glass properties during a substitution of S by Se in $Ge_{28}Sb_{12}S_{60-x}Se_x$ glass network," J. Non-Cryst. Solids **358**(15), 1740–1745 (2012).

16. D. Lezal, "Chalcogenide glasses- survey and progress," J. Optoelectron. Adv. Mater. **5**(1), 23–34 (2003).

17. V. G. Borisevich, V. V. Voitsekhovsky, I. V. Scripachev, V. G. Plotnichenko, and M. F. Churbanov, "Investigation of the influence of extrinsic hydrogen on the optical properties of chalcogenide glasses in the system As-Se," Vysokochist. Vesch. **1**, 65 (1991).

18. M. F. Churbanov, G. E. Snopatin, V. S. Shiryaev, V. G. Plotnichenko, and E. M. Dianov, "Recent advances in preparation of high-purity glasses based on arsenic chalcogenides for fiber optics," J. Non-Cryst. Solids **357**(11-13), 2352–2357 (2011).

19. E. V. Karaksina, V. S. Shiryaev, T. V. Kotereva, and M. F. Churbanov, "Preparation of high-purity Pr(3+) doped Ge–Ga–Sb–Se glasses with intensive middle infrared luminescence," J. Lumin. **170**(1), 37–41 (2016).

20. V. Shiryaev and M.F. Churbanov, "Preparation of high-purity chalcogenide glasses," Chapter 1 in Chalcogenide Glasses, J.L Adam and X. Zhang, eds. (Woodhead Publishing Limited, 2014).

21. G. E. Snopatin, V. S. Shiryaev, V. G. Plotnichenko, E. M. Dianov, and M. F. Churbanov, "High-purity chalcogenide glasses for fiber optics," Inorg. Mater. **45**(13), 1439–1460 (2009).

22. W. L. Jolly and W. M. Latimer, "The Equilibrium $Ge_{(s)} + GeO_{2(s)} = 2GeO_{(g)}$. The Heat of Formation of Germanic Oxide," J. Am. Chem. Soc. **74**(22), 5757–5758 (1952).

23. S. Pizzini, *Physical Chemistry of Semiconductor Materials Processing* (John Wiley & Sons, Ltd. 2015), Chap. 5.

24. D. Furniss and A.B. Seddon, "Thermal Analysis of Inorganic Compound Glasses and Glass-Ceramics," Chap. 10 in Principles and Applications of Thermal Analysis, P. Gabbott, ed. (Blackwell Publishing Ltd, 2008).

25. S. D. Savage, C. A. Miller, D. Furniss, and A. B. Seddon, "Extrusion of chalcogenide glass preforms and drawing to multimode optical fibers," J. Non-Cryst. Solids **354**(29), 3418–3427 (2008).

26. Z. Tang, V. S. Shiryaev, D. Furniss, L. Sojka, S. Sujecki, T. M. Benson, A. B. Seddon, and M. F. Churbanov, "Low loss Ge-As-Se chalcogenide glass fiber, fabricated using extruded preform, for mid-infrared photonics," Opt. Mater. Express **5**(8), 1722–1737 (2015).

27. I. Vurgaftman, R. Weih, M. Kamp, J. R. Meyer, C. L. Canedy, C. S. Kim, M. Kim, W. W. Bewley, C. D. Merritt, J. Abell, and S. Höfling, "Interband Cascade Lasers," J. Phys. D: Appl. Phys. **48**(12), 123001 (2015).

28. M. Kim, C. S. Kim, C. L. Canedy, W. W. Bewley, C. D. Merritt, I. Vurgaftman, and J. R. Meyer, "Recent advances of interband cascade lasers and LEDs," *Proc. SPIE* 10939 (2019).

29. Y. Fang, D. Jayasuriya, D. Furniss, Z. Q. Tang, Ł Sojka, C. Markos, S. Sujecki, A. B. Seddon, and T. M. Benson, "Determining the refractive index dispersion and thickness of hot-pressed chalcogenide thin films from an improved Swanepoel method," Opt. Quantum Electron. **49**(7), 237 (2017).

30. T. Wang, W. H. Wei, X. Shen, R. P. Wang, B. Luther-Davies, and I. Jackson, "Elastic transition thresholds in Ge–As(Sb)–Se glasses," J. Phys. D: Appl. Phys. **46**(16), 165302 (2013).

31. J. A. Harrington, *Infrared Fibers and Their Applications* (SPIE Press, 2004).

32. B. Zhang, W. Guo, Y. Yu, C. Zhai, S. Qi, A. Yang, L. Li, Z. Yang, R. Wang, D. Tang D, G. Tao, and B. Luther-Davies, "Low loss, high NA chalcogenide glass fibers for broadband mid-infrared supercontinuum generation," J. Am. Ceram. Soc. **98**(5), 1389–1392 (2015).

33. G. E. Snopatin, M. F. Churbanov, A. A. Pushkin, V. Gerasimenko, E. Dianov, and V. Plotnichenko, "High purity arsenic-sulfide glasses and fibers with minimum attenuation of 12 dB/km," Optoelectronics and advanced materials-rapid communications **3**(7), 669–671 (2009).